



## Does water column stratification influence the vertical distribution of microplastics?<sup>☆</sup>

Kuddithamby Gunaalan<sup>a,c,\*</sup>, Rodrigo Almeda<sup>a,b</sup>, Alvise Vianello<sup>c</sup>, Claudia Lorenz<sup>c,d</sup>, Lucian Iordachescu<sup>c</sup>, Konstantinos Papacharalampos<sup>c</sup>, Torkel Gissel Nielsen<sup>a</sup>, Jes Vollertsen<sup>c</sup>

<sup>a</sup> National Institute of Aquatic Resource, Technical University of Denmark, Denmark

<sup>b</sup> EOMAR, ECOAQUA, University of Las Palmas of Gran Canaria, Spain

<sup>c</sup> Department of the Built Environment, Aalborg University, Denmark

<sup>d</sup> Department of Science and Environment, Roskilde University, Denmark

### ARTICLE INFO

#### Keywords:

Microplastics  
Vertical distribution  
Pycnocline  
Water stratification  
FPA- $\mu$ FTIR-Imaging

### ABSTRACT

Microplastic pollution has been confirmed in all marine compartments. However, information on the sub-surface microplastics (MPs) abundance is still limited. The vertical distribution of MPs can be influenced by water column stratification due to water masses of contrasting density. In this study, we investigated the vertical distribution of MPs in relation to the water column structure at nine sites in the Kattegat/Skagerrak (Denmark) in October 2020. A CTD was used to determine the stratification and pycnocline depth before sampling. Plastic-free pump-filter sampling devices were used to collect MPs from water samples (1–3 m<sup>3</sup>) at different depths. MPs concentration (MPs m<sup>-3</sup>) ranged from 18 to 87 MP m<sup>-3</sup> (Median: 40 MP m<sup>-3</sup>; n = 9) in surface waters. In the mid waters, concentrations ranged from 16 to 157 MP m<sup>-3</sup> (Median: 31 MP m<sup>-3</sup>; n = 6), while at deeper depths, concentrations ranged from 13 to 95 MP m<sup>-3</sup> (Median: 34 MP m<sup>-3</sup>; n = 9). There was no significant difference in the concentration of MPs between depths. Regardless of the depth, polyester (47%), polypropylene (24%), polyethylene (10%), and polystyrene (9%) were the dominating polymers. Approximately 94% of the MPs fell within the size range of 11–300  $\mu$ m across all depths. High-density polymers accounted for 68% of the MPs, while low-density polymers accounted for 32% at all depths. Overall, our results show that MPs are ubiquitous in the water column from surface to deep waters; we did not find any impact of water density on the depth distribution of MPs despite the strong water stratification in the Kattegat/Skagerrak.

### 1. Introduction

The accumulation and effects of plastic pollution in the ocean are of global environmental concern. Understanding the fate and processes affecting the distribution of MPs in the ocean is crucial to evaluating the impacts of plastic litter on marine ecosystems. In recent years, microplastics (MPs) in surface waters have been extensively examined by using nets, mainly the Manta net (Cózar et al., 2014; Setälä et al., 2016; Pasquier et al., 2022) and pump-filtering devices (e.g., Rist et al., 2020; Gunaalan et al., 2023a). It is estimated that floating plastics only account for less than 1% of the total plastic entering the ocean (Cressey, 2016), and there is increasing evidence that the seafloor is a sink for MPs (Van Cauwenbergh et al., 2013; Woodall et al., 2014; Martin et al., 2022; Simon-Sánchez et al., 2022; Fagiano et al., 2023). However, there is

limited understanding regarding concentration, vertical distribution, and characteristics of sub-surface MPs (Thompson et al., 2004; Doyle et al., 2011; Kanhai et al., 2018; Zhao et al., 2023).

Large-scale oceanographic factors like ocean currents influence the horizontal and vertical distribution of MPs in the ocean (Law et al., 2010; Zobkov et al., 2019) and mesoscale processes such as eddies, convective flows, and upwelling (Brach et al., 2018; Díez-Minguito et al., 2020; Vega-Moreno et al., 2021). Vertical water mixing also affects the distribution of both positively and negatively buoyant MPs (Liu et al., 2020; Uurasjärvi et al., 2021). Several studies found that water column stratification influences the distribution of MPs (Wu et al., 2019; Zhou et al., 2021), even causing the accumulation of MPs in thin sub-surface water layers (Uurasjärvi et al., 2021). For instance, Uurasjärvi et al., 2021 found 1000 times more MPs at the beginning of the

<sup>☆</sup> This paper has been recommended for acceptance by Eddy Y. Zeng.

\* Corresponding author. National Institute of Aquatic Resources (DTU Aqua), Technical University of Denmark, Kemitorvet, Kongens Lyngby, Denmark.

E-mail address: [guku@aqu.dtu.dk](mailto:guku@aqu.dtu.dk) (K. Gunaalan).

thermocline than in the other water layers in Baltic waters. However, other studies have found a less clear/no influence of water stratification on MP vertical distribution (Eo et al., 2021; Zhou et al., 2021).

The sinking and distribution of MPs in the water column are also influenced by the size and density of the particles (Kowalski et al., 2016; Borges-Ramírez et al., 2020; Shamskhany et al., 2021; Reisser et al., 2015) found that smaller plastic particles are more susceptible to vertical transport, with plastic concentrations dropping exponentially with water depth in the North Atlantic Gyre. MPs with a density lower than seawater, such as polypropylene and polyethylene, are expected to float on surface waters. However, biological interactions, e.g., ingestion and integration in fast-sinking zooplankton fecal pellets (Kvale et al., 2020a; Kvale et al., 2020b) and aggregation of MPs to biological detritus like marine snow (Michels et al., 2018; Zhao et al., 2018) can accelerate the sinking rates of MPs (Porter et al., 2018), which can explain the high occurrence of low-density MPs in subsurface waters and sediments (Song et al., 2018). However, little is still known about the characteristics of MPs in subsurface waters at different depths, particularly for small MPs fractions ( $<300\ \mu\text{m}$ ).

The Kattegat and the Skagerrak connect the North Sea with the brackish Baltic Sea. The hydrography of the Kattegat is characterized by an upper layer of lower saline surface water originating from the Baltic Sea and a deeper layer of higher saline water from the Skagerrak. These two water masses are separated by a strong pycnocline (Richardson, 1996; Matthews et al., 1999). This strong stratification makes Kattegat a good model area to investigate the influence of water density on the vertical distribution of MPs and to identify sub-surface water layers of

the potential accumulation of plastic pollution. Here, we quantify and characterize the MPs  $>10\ \mu\text{m}$  in different water layers in Kattegat/Skagerrak basins (Denmark) to evaluate the influence of the water column stratification on the vertical distribution of MPs. We hypothesized that the density of the water masses affects the vertical distribution and composition of MPs.

## 2. Materials and methods

### 2.1. Study area and sampling devices

The sampling was conducted in October 2020 onboard the R/V DANA (DTU Aqua), covering twelve locations in the Kattegat Sea and two in the Skagerrak (Gunaalan et al., 2023a). However, this study specifically focuses on the water column samples collected from nine stations: stations (St) 1, 4, 5, 6, 8, 9, 10, 12, and 14. (Fig. 1A). The selected stations cover coastal and offshore waters with different levels of water stratification, including the Northern and Southern regions of the Kattegat, where higher concentrations of MPs were found in surface waters (Gunaalan et al., 2023a). Among these selected stations, seven are situated in the typical areas of Kattegat. Station 4 is located in the Southwestern part, and stations 5 and 6 are in the Southern region. Stations 8, 9, and 10 are located eastward in an area connected to the Western Baltic Sea. Additionally, station 12 is in the central area of the Kattegat. Finally, two stations (1 and 12) are located in a deeper area within the Skagerrak region, which connects to the North Sea. All stations were analyzed for the surface layer, and stations 5, 6, 8, 10, 12 and

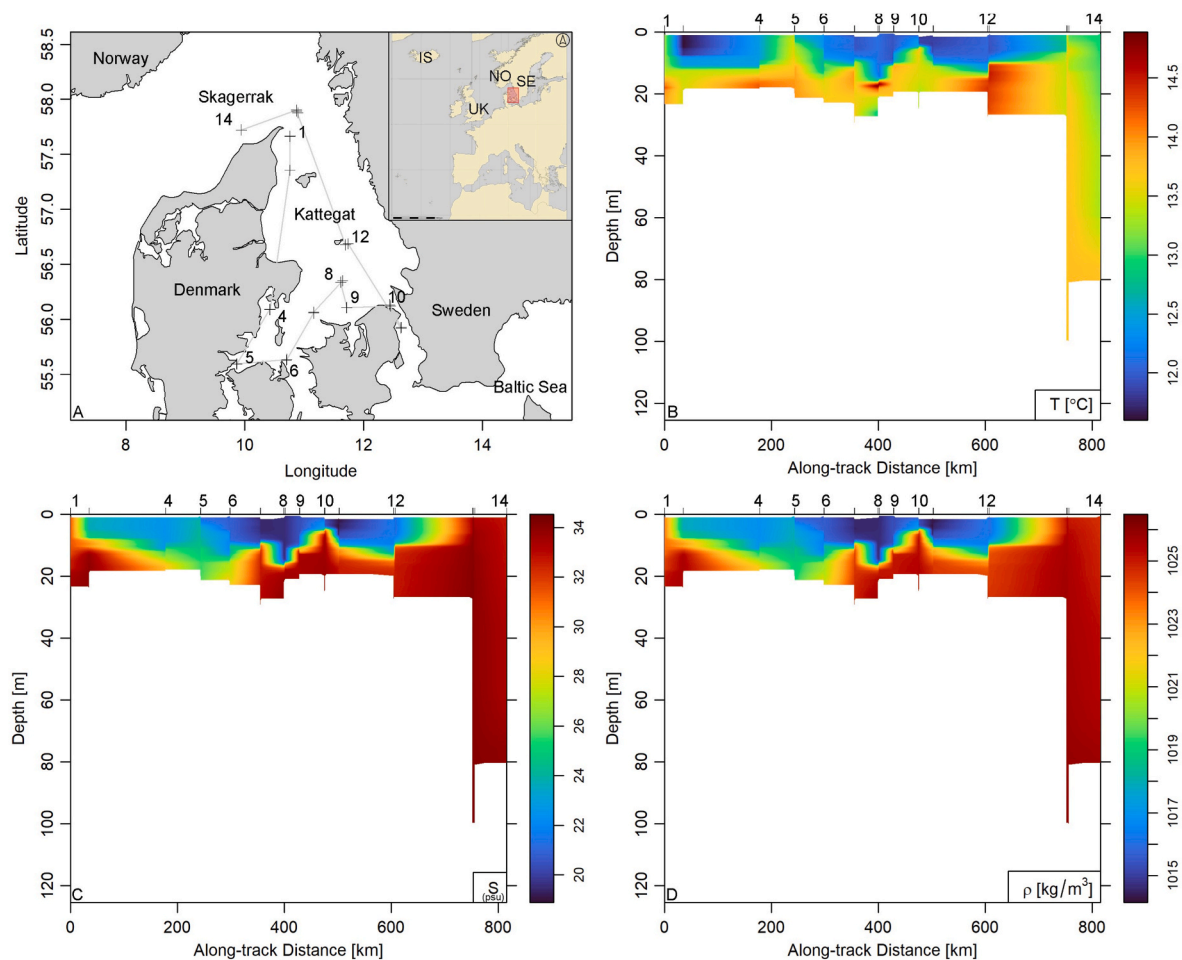


**Fig. 1.** Map of study locations (St- 1, 4, 5, 6, 8, 9, 10, 12, 14) (A) and the vertical profiles of temperature (B), salinity (C), and density (D) in the study area during the sampling period.

14 were studied for mid-layer (Pycnocline). Deep layer samples were analyzed from stations 1, 4, 5, 6, 9, 10, 12 and 14. The stations were selected to cover different water masses. Temperature, salinity, and fluorescence measurements were taken from the surface to a depth of 1 m above the seafloor using a Sea-Bird CTD System (Sea-Bird Scientific SBE 9). MPs larger than 10  $\mu\text{m}$  were collected using a plastic-free pump-filter device called “AAU-KRAKEN”. The AAU-KRAKEN consists of a steel cylinder housing a borehole deep-well pump and six attached filtering units (UFO), derived from the system used by Rist et al., 2020, Gunaalan et al., 2023a; Liu et al., 2023. Each UFO holds a 10  $\mu\text{m}$  steel filter measuring 167 mm in diameter. Water passes through these UFO units and is expelled through the device’s outlet, where a flowmeter measures the filtered water. The device, powered by lithium batteries held in a sealed steel housing, was deployed from the CTD deck, and controlled via the oceanographic winch, allowing it to filter around 3  $\text{m}^3$  of water in 30 min at each deployment.

## 2.2. Sample preparation, MPs detection and data analysis

The particle-enriched steel filters collected at each station by the “Kraken” were subsequently processed according to the protocol outlined in Gunaalan et al., 2023a). Briefly, the extraction of MPs from the filters involved several main steps. Firstly, the filters were soaked in sodium dodecyl sulphate (SDS), which ensures the solubilizing of samples and facilitates the breakdown of macromolecules in the samples. Next, enzymatic digestion was carried out using protease and cellulase enzymes to denature the proteins and cellulose materials in the samples. Subsequently, Fenton oxidation was conducted to further degrade the remaining organic matter and improve the MPs’ separation. A size fractionation was then performed to segregate the MPs  $>300 \mu\text{m}$  using a metal sieve. Finally, a density separation using sodium polytungstate (SPT,  $\rho = 1.7 \text{ g cm}^{-3}$ ) was carried out to extract the MPs from any inorganic material. An aliquot representing 50–60% of the sample was deposited onto multiple Zinc Selenide (ZnSe) windows ( $\text{Ø} = 13 \text{ mm}$ ; thickness = 2 mm). Subsequently, the entire active surface of the ZnSe window ( $\text{Ø} = 11 \text{ mm}$ ) was analyzed by Focal plane array (FPA) based micro Fourier transform Infrared Spectroscopy ( $\mu\text{FTIR}$ ) Imaging using the instrumental parameters described in Gunaalan et al., 2023a, 2023b.

The spectral data obtained from  $\mu\text{FTIR}$ -Imaging were analyzed using a freeware siMPle (<https://simple-plastics.eu/>), which allows automated analysis of large hyperspectral data sets (Primpke et al., 2020). Ultimately, we obtained details on the size (length, width, and Feret diameter), polymer type, and estimated mass of the particle from siMPle software encompassing a total of 1234 MPs across all depths. The mass estimates were computed by considering the volume of the particles, assuming an ellipsoid shape, and incorporating the density specific to the respective polymer types (Simon et al., 2018; Liu et al., 2019; Rist et al., 2020; Gunaalan et al., 2023a). The distinction between the shapes of the MPs was performed by evaluating the ratio between the length and width of the particles. Fibers were classified as particles with a length-to-width ratio greater than three, whereas fragments were defined as those with a ratio less than three (World Health Organization, 1997; Vianello et al., 2019).

## 2.3. Quality control and quality assurance

Quality control and quality assurance measures were implemented as outlined in Gunaalan et al., 2023a, ensuring a comprehensive contamination control approach. Briefly, all materials were muffled at 500  $^{\circ}\text{C}$ , and wrapped in aluminum foil until use. All chemical solutions used for sample processing were filtered over 0.7  $\mu\text{m}$  GF/F filters. Samples were prepared in a laminar flow bench, and cotton laboratory coats were always worn. Moreover, representative samples were taken from all the possible critical cross-contamination points onboard the vessel, including the ship’s paints. Two types of blanks were employed to assess contamination in different stages of the sampling and sample

preparation processes. The “air blanks” were used during the “Kraken” sampling to evaluate airborne contamination (Gunaalan et al., 2023a), while “procedural blank” were carried out in the laboratory during sample preparation to assess the contamination at that stage.

## 2.4. Data processing and statistical analysis

The number of MPs was scaled up to the entire respective sample volumes contained in the vials (5 mL) based on the  $\mu\text{FTIR}$ -scanned fraction and corrected for cross-contamination recorded in “procedural” and “air” blanks. Descriptive statistics and graphical illustrations were computed using R software (R 4.2.1).

To evaluate the diversity and similarity of polymers in the studied depths, we computed three metrics: Shannon-Wiener index  $H'$  (natural logarithm base)(Lorenz et al., 2019; Sun et al., 2021), richness, and the Sørensen’s coefficient for similarity.

$$\text{Shannon – Wiener index}(H') = -\sum\{p_i \times \ln(p_i)\} \quad \text{eq (1)}$$

$$\text{Polymer richness}(S) = \text{Number of polymers detected} \quad \text{eq (2)}$$

$$\text{Sørensen Coefficient} = \frac{2C}{S1+S2} \quad \text{eq (3)}$$

Where,  $p_i$  = proportion of total polymers represented by each polymer type.

$C$  = Number of polymers common in the two different depth.

$S1$  = Total number of polymers at depth 1.

$S2$  = Total number of polymers at depth 2.

## 3. Results

### 3.1. Oceanographic features

The CTD data showed depth differences in salinity, temperature, and density (Fig. 1). In the Kattegat, the surface layer (0–15m) exhibited a consistent temperature (11.9–13.3  $^{\circ}\text{C}$ ), although significant salinity level changes from 19.5 to 32.8 psu across the pycnocline. In addition, notable changes in temperature and salinity were observed in deeper waters (St-14), causing the formation of distinct water masses/stratification. In the case of the Skagerrak (St-14), the temperature (12.91–13.7  $^{\circ}\text{C}$ ) and salinity (32.8–33.9 psu) were relatively higher than the other stations (Fig. 1). Overall, a pronounced stratification was observed in the water layers. This prominent differentiation in density clearly showed the characteristic layering within the study area.

### 3.2. Blank correction

The air blanks and procedural blank contained a median MPs concentration and estimated mass of 1.25 MPs and 0.10  $\mu\text{g}$  per sample, respectively. The polymer composition of MPs in the blanks was 69% polyester, 18% acrylic paint, 6%, polyvinyl chloride, 2% polyamide, 2% polystyrene, and 1% vinyl chloride copolymer, PAN acrylic fiber, and polyethylene. The results were adjusted for contamination by deducting the median contribution of each polymer identified in the blank samples from the MPs number and mass estimates.

### 3.3. Vertical distribution of MP abundance and mass in the water column

The MPs concentration and distribution were heterogenic, varying among sites and depths (Table 1). The concentration of MPs in surface waters was relatively high in St.1 (87  $\text{MP m}^{-3}$ ), St.14 (62  $\text{MP m}^{-3}$ ), and St.10 (57  $\text{MP m}^{-3}$ ). In the mid-water samples, St.5 and 12 had the higher concentration MPs (157  $\text{MP m}^{-3}$ , and 66  $\text{MP m}^{-3}$  respectively), while in the deep water MPs concentration was higher in St.5, 4, and 9 (95  $\text{MP m}^{-3}$ , 82  $\text{MP m}^{-3}$  and 68  $\text{MP m}^{-3}$  respectively) (Fig. S1). The concentrations of MPs (mean  $\pm$  SD) in the surface, mid, and bottom waters

**Table 1**

Summary of MPs size and mass observed at different depths in the study area (n, given the number of stations where samples were taken).

Vertical layer	MPs Abundance (MPs m <sup>-3</sup> )			MPs Shape	MPs Size and Mass					
	Range	Median	Mean ± SD		Length (µm)		Width (µm)		Mass (µg)	
					Median	Mean ± SD	Median	Mean ± SD	Median	Mean ± SD
Surface (n = 9)	18–87	40	41 ± 24	Total MPs	76.6	139.4 ± 187.5	27.6	37.4 ± 37.7	22.2	0.87 ± 7.84
				Fragments	52.4	74.6 ± 81.5	27.5	35.4 ± 30.0	0.02	0.29 ± 2.26
				Fibers	151.7	228.0 ± 246.8	27.7	40.2 ± 46.3	0.06	1.66 ± 11.76
Mid (n = 6)	16–157	31	53 ± 54	Total MPs	67.6	104.6 ± 123.3	27.8	32.1 ± 23.3	0.02	0.12 ± 0.69
				Fragments	54.5	64.1 ± 47.4	29.3	33.7 ± 25.7	0.02	0.11 ± 0.80
				Fibers	145.2	201.4 ± 181.6	24.3	28.2 ± 15.4	0.04	0.13 ± 0.30
Deep (n = 8)	13–95	35	47 ± 29	Total MPs	66.5	96.7 ± 83.7	27.6	33.4 ± 21.7	0.02	0.09 ± 2.48
				Fragments	55.2	66.6 ± 46.2	28.1	34.1 ± 22.0	0.01	0.07 ± 2.35
				Fibers	157.8	179.9 ± 105.6	25.7	31.4 ± 20.9	0.04	0.13 ± 0.28

were  $41 \pm 24$  (Median = 40; n = 9),  $53 \pm 54$  (Median = 31; n = 6), and  $47 \pm 29$  (Median = 35; n = 8) MPs m<sup>-3</sup>, respectively (Table 1). In general, due to the high variability, no significant difference was found between surface, midwater, and deep water (Kruskal-Wallis test,  $p > 0.05$ ). Similarly, the mean concentration of MP mass estimates in the surface water was  $32.7 \pm 64 \mu\text{g m}^{-3}$  (Median:  $6.2 \mu\text{g m}^{-3}$ ). Mid-water samples had an average concentration of  $6.1 \pm 3.6 \mu\text{g m}^{-3}$  (Median:  $6.5 \mu\text{g m}^{-3}$ ), while the deep-water samples showed a mean concentration of  $4.1 \pm 5.5 \mu\text{g m}^{-3}$  (with a median of  $2.1 \mu\text{g m}^{-3}$ ). Remarkably, the surface water of stations 1 and 6 exhibited a higher mass concentration compared to all other samples (Fig. S1). These two stations contained outliers where few single particles contributed to more than half of the total mass compared to the other particles.

The pycnocline depth varied among the stations (Fig. 2), and no correlation was observed between the MPs abundance and vertical water density (Pearson correlation,  $p > 0.05$ ,  $R^2 = 0.0006$ ). Among the surveyed stations, station 9 exhibited the highest salinity gradient of  $4.33 \text{ psu m}^{-1}$  at the halocline depths, followed by station 8 with a gradient of  $3.25 \text{ psu m}^{-1}$ . Similarly, for the temperature gradient at the thermocline depths, station 9 had the highest value of  $0.60 \text{ }^\circ\text{C m}^{-1}$ , followed by station 8 with a gradient of  $0.47 \text{ }^\circ\text{C m}^{-1}$ . In contrast, station 14 displayed the lowest gradient among all stations, with  $0.01 \text{ psu m}^{-1}$

at the halocline and  $0.01 \text{ }^\circ\text{C m}^{-1}$  at the thermocline depths (Fig. S2).

#### 3.4. Polymer composition of MPs at different depths

The polymer composition in terms of numbers for each station and sampling depth is shown in Fig. 3A. Overall, 21 different types of polymers were identified (Fig. 3A). Polymer (species) diversity was higher at St 5 midwater ( $H = 1.92$ ), and the lowest recorded in St 14 surface water and St 10 midwater ( $H = 0.59$ ) (Table S1). The analysis using the Sørensen similarity index indicated that St 5, 6, and 12 showed higher similarity values between mid and deep-water layers (Table S1). This suggests a greater variety of polymers present in these water layers. Conversely, the similarity of polymers was relatively low between the surface and mid-layers (Table S1). The polymer compositions at each station were generally comparable across vertical layers, and there was no observable trend of increasing or decreasing polymer proportions with the water depth (Fig. 3A). Polyester, polypropylene, and polyethylene emerged as the most dominant polymers across the vertical layers of the study sites; however, it is worth noting that polyester was absent in the deep layers of station 14, and no polypropylene was identified in station 8 (Fig. 3A). When we compared the composition of polymer types among depths by combining data from different sites, we

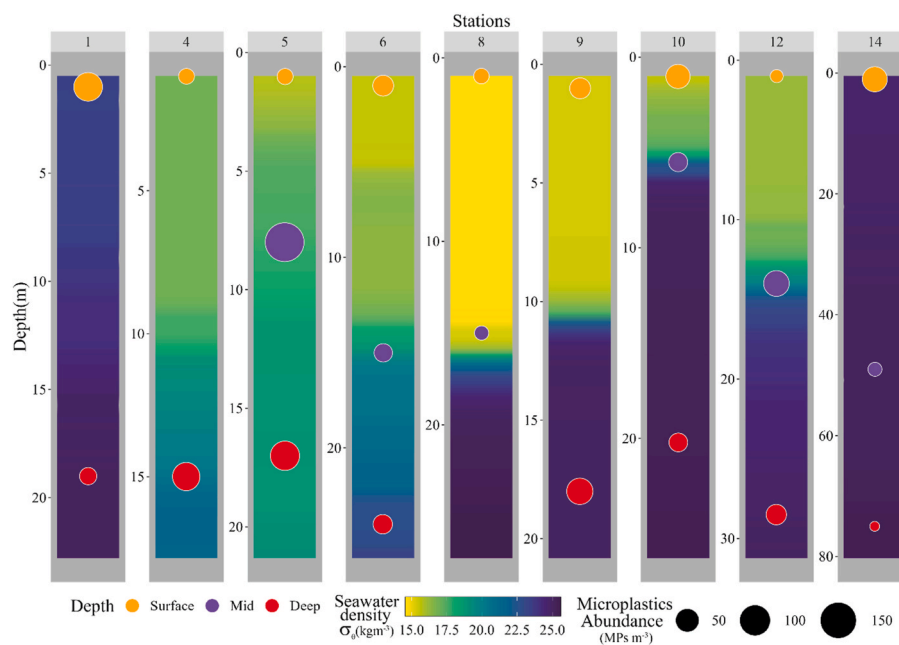


**Fig. 2.** MPs abundance at the surface, mid and deep water in the selected study sites of Danish marine waters. Each column represents the interpolated vertical seawater density ( $\sigma_0$ ) distribution in each study site (range  $\sigma_0$  14.6–25.3 kg m<sup>-3</sup>), the different colors of the circle indicate the different depths of the water column (surface, mid and deep water) and the circle size illustrates the abundance of MPs (MPs m<sup>-3</sup>) at the sampling depths. (For interpretation of the references to color in this figure legend, the reader is referred to the Web version of this article.)

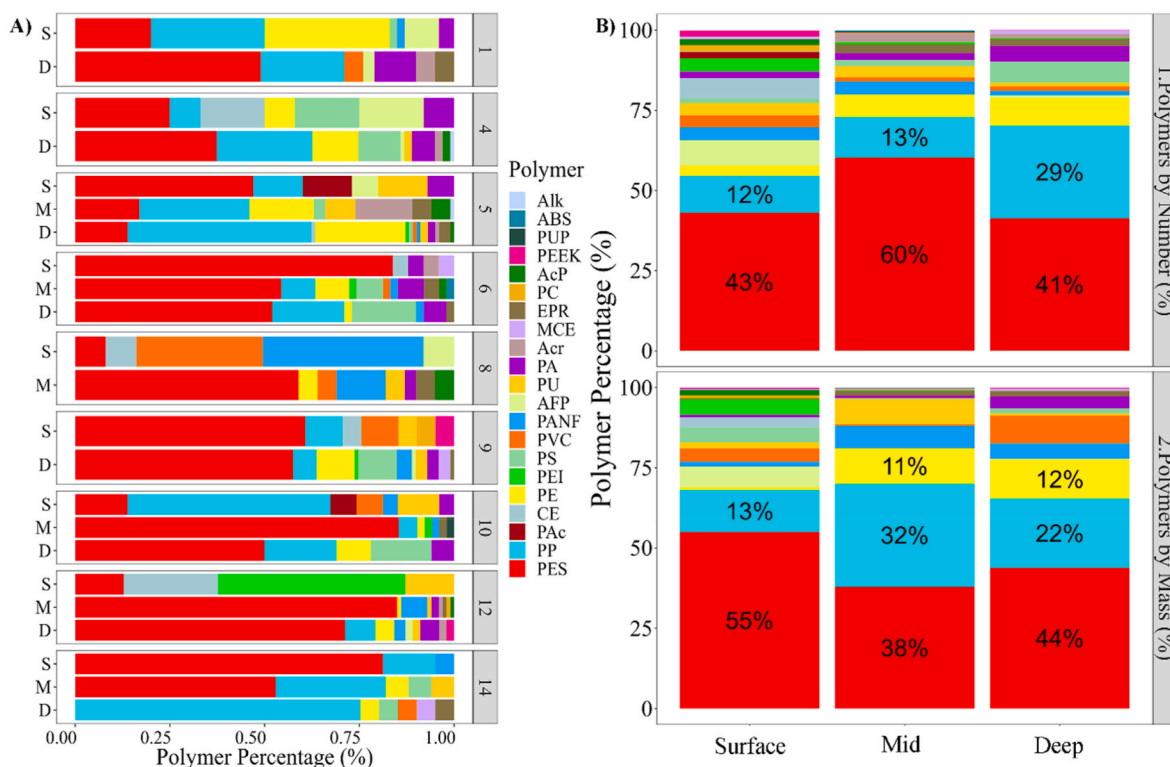


**Fig. 3.** A) Average percentage of polymer composition in the different depths combining all the sites. B) The upper panel displays the polymer composition percentages based on the number of MPs, while the lower panel shows the estimated polymer composition percentages based on mass estimates. (ABS: Acrylonitrile butadiene styrene, AcP: Acrylic paint, Acr: Acrylic, AFP: Antifouling paint, Alk: Alkyd, CE: Cellulose ester, EPR: Epoxy phenoxy resin, MCE: Modified cellulose ester, PA: Polyamide, PANF: PAN acrylic fiber, PC: Polycarbonate, PE: Polyethylene, PEEK: Polyether ether ketone, PEI: Polyethylenimine, PAC: Polyacrylamide, PES: Polyester, PP: Polypropylene, PS: Polystyrene, PU: Polyurethane, PUP: Polyurethane paint, PVC: Polyvinylchloride).

observed that polyester, was the most prevalent polymer in the three water layers, accounting for 41–60% of the samples. This was followed by polypropylene 12–29% and polyethylene 3–9%. The remaining polymers comprised 20–42% of the sample (Fig. 3B). Furthermore, polyester and polypropylene collectively accounted for over 50% of both number and mass estimates (Fig. 3B).

### 3.5. Density, size and shape of MPs

The categorization of polymers into low-density (LD;  $<1.02 \text{ g cm}^{-3}$ ) and high-density (HD;  $>1.02 \text{ g cm}^{-3}$ ) was determined based on their theoretical density relative to seawater. Among the high-density polymers, a further classification was made by creating two categories, HD1 ( $1.02\text{--}1.2 \text{ g cm}^{-3}$ ) and HD2 ( $>1.2 \text{ g cm}^{-3}$ ). (Table S2). No vertical gradient was observed in terms of polymer density and compositional proportion (Fig. 4A). Low-density polymers (LD) were distributed throughout the water column, including deep waters, accounting for an average proportion of 40%, while HD1 and HD2 polymers constituted 16% and 44%, respectively. Overall, the study area exhibited a composition of 32% LD and 68% HD polymers across all depths (Fig. 4A).

Moreover, MPs were categorized based on their length into five groups: 11–50  $\mu\text{m}$ , 51–100  $\mu\text{m}$ , 101–200  $\mu\text{m}$ , 201–300  $\mu\text{m}$  and  $>300 \mu\text{m}$ . It was observed that MPs with lengths below 100  $\mu\text{m}$  were more abundant in mid and deep waters, accounting for 70% each, while surface water contained 48% of this size category. Interestingly, all the stations showed that MPs with sizes below 100  $\mu\text{m}$  accounted for more than 50% at all paths, except for stations 6 and 9 in the surface water and station 10 in the mid-water layer (Fig. 4B).

The length of MPs did not show significant differences between the mid-depth and deep layers, however both exhibited significant differences when compared to the surface layer (Fig. 5). In particular, the

percentage of MPs with a size less than 300  $\mu\text{m}$  was recorded as 90%, 94%, and 95% for the surface, mid-depth, and deep-depth layers, respectively (Fig. 5).

MPs in both deep and mid-water samples were predominantly fragments at all stations, except for St 10 in the mid-water samples, which was primarily dominated by fibers (69%). However, in surface waters, stations 6, 9 and 14 exhibited a dominance of fibers with percentages of 70%, 57%, and 82%, respectively. Additionally, the ratio of fiber to fragment decreased with increasing depth. Specifically, the ratio was 0.73 in surface waters, 0.42 in mid-depth, and 0.35 in deep waters.

In order to achieve a comprehensive and unified understanding of MPs found at different depths, Fig. 6 highlights the interrelationships amongst their diverse characteristics, including size, shape, polymer type, and density of the polymers. For instance, within the deep-depth layer, the prevailing composition of small MPs (95.4%) fragments (73.1%) primarily comprises polyester (21.4%) and polypropylene (23.4%) exhibiting high and low densities, respectively (Fig. 6). Furthermore, small MPs fragments were found in surface, mid, and deep water at 56.7%, 70.0%, and 73.1%, respectively (Fig. 6).

## 4. Discussion

### 4.1. Distribution of MPs in the water column in the ocean

Multiple factors, including mesoscale convective flows, hydrodynamic stability, precipitation, sedimentation rate, flow rate, and depth of the water bodies can influence the distribution and concentration of MPs in the aquatic systems (Vega Moreno et al., 2021; Lee et al., 2013). In our study, we found a positive relationship between the concentration of MPs in the water column and coastal proximity, suggesting an influence of land sources on the measured MP concentrations (Fig. S3). On the other hand, we did not find any influence of wind speed on the

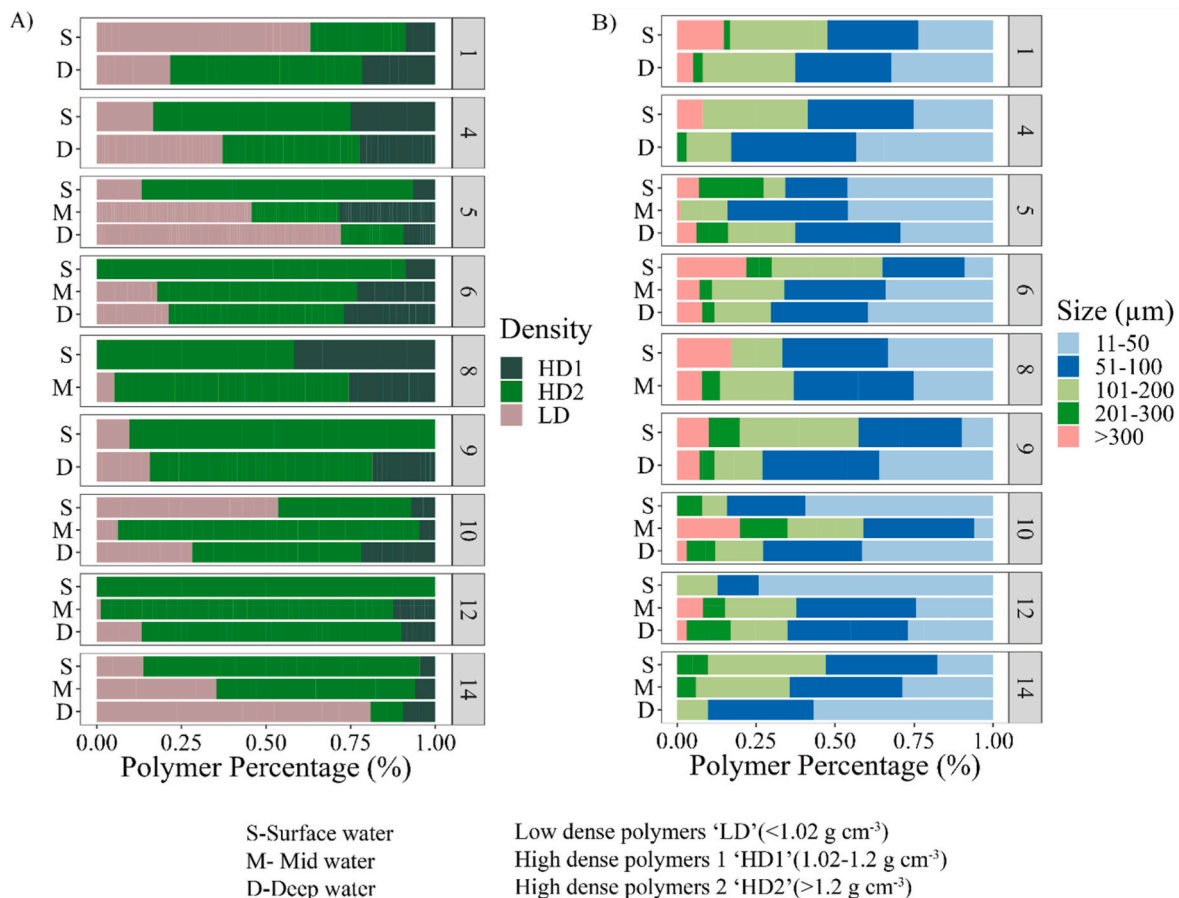


**Fig. 4.** Proportion (%) of MPs according to their density (A) and size (B) at study sites. High-density polymers (HD) were categorized into HD1 (1.02–1.2 g cm<sup>-3</sup>) and HD2 (>1.2 g cm<sup>-3</sup>). The densities of low density (LD) MPs are <1.02 g cm<sup>-3</sup>.

concentration of MPs in the studied stations (Fig. S3). Regarding the vertical distribution of MPs, the present study provides the first quantification of the vertical distribution of MPs in Danish marine waters across a pycnocline. The vertical distribution of MPs in the ocean varies regionally and different patterns have been reported, from a strong decrease to an increase in MP abundance with depth (Reisser et al., 2015; Song et al., 2018; Choy et al., 2019; Tekman et al., 2020). An exponential decrease in MP concentration has been found in the North Atlantic subtropical gyre (Reisser et al., 2015), but other studies have found a higher accumulation of MPs in subsurface waters. For instance, higher concentrations of MPs compared to surface water were found in mesopelagic waters (200–600) in the offshore waters of Monterey Bay (Choy et al., 2019), mid and bottom depths in Korean coastal waters (Song et al., 2018) and the beginning of the pycnocline, 10–30 m in the Baltic (Uurasjärvi et al., 2021). In contrast, except for one station at the Fram Strait from HAUSGARTEN observatory, the near-surface samples from all stations had the highest MPs concentrations (Tekman et al., 2020). These studies and our results for Danish waters confirm that although the vertical distribution pattern of MPs can vary regionally, MPs are not restricted to surface waters but distributed through the entire water column. The current global estimations of plastic pollution in the ocean are mainly based on buoyant MPs >300  $\mu\text{m}$  sampled in surface waters (Cózar et al., 2014; Eriksen et al., 2014; van Sebille et al., 2015). The quantification of the vertical distribution of MPs, including small-size fractions as conducted here, can help to estimate the amount of plastics in the ocean and their fate and potential impacts on the pelagic systems.

#### 4.2. Influence of water column stratification on the vertical distribution of MPs

Water stratification is one of the significant physical factors that influence the distribution and sinking rates of MPs within the water column (Liu et al., 2020; Uurasjärvi et al., 2021). In the case of the Kattegat region, the water column is strongly stratified (Pedersen, 1993; Nielsen, 2005; Bendtsen et al., 2009; Lehmann et al., 2022; Ni et al., 2023). The pycnocline can act as a density barrier and hinder the sinking of MPs from surface water to deep waters (Reisser et al., 2015; Isobe et al., 2017). There are studies which have found that MPs are trapped at the beginning of the pycnocline in the Baltic Sea, showing that the change in water density from low to high salinity affects the sinking of MPs within the water column (Zobkov et al., 2019; Uurasjärvi et al., 2021; Zhou et al., 2021). In our study area, we observed no significant difference in the concentration of MPs among different water masses despite the strong pycnocline present in the Kattegat (Figs. S2 and S4). These results align with previous studies conducted by Eo et al. (2021) in Korean waters, Zhao et al., 2022 in the South Atlantic Gyre, and Parać et al., 2022 in the Eastern Adriatic coast of Croatia. Our sampling in mid-waters was generally in the middle of the pycnocline (Fig. 2) and not at the beginning of the pycnocline, where the accumulation of MPs has been observed in previous studies in the Baltic (Zobkov et al., 2019; Uurasjärvi et al., 2021; Zhou et al., 2021). Thus, it may be possible that MPs are concentrated only in very thin layers at the beginning of the pycnocline. To detect patches and thin layers of MPs in marine waters, there is a need for increased resolution of vertical profiles.

Besides the physical processes and the characteristics of MPs, other factors like biological interactions can influence the vertical distribution

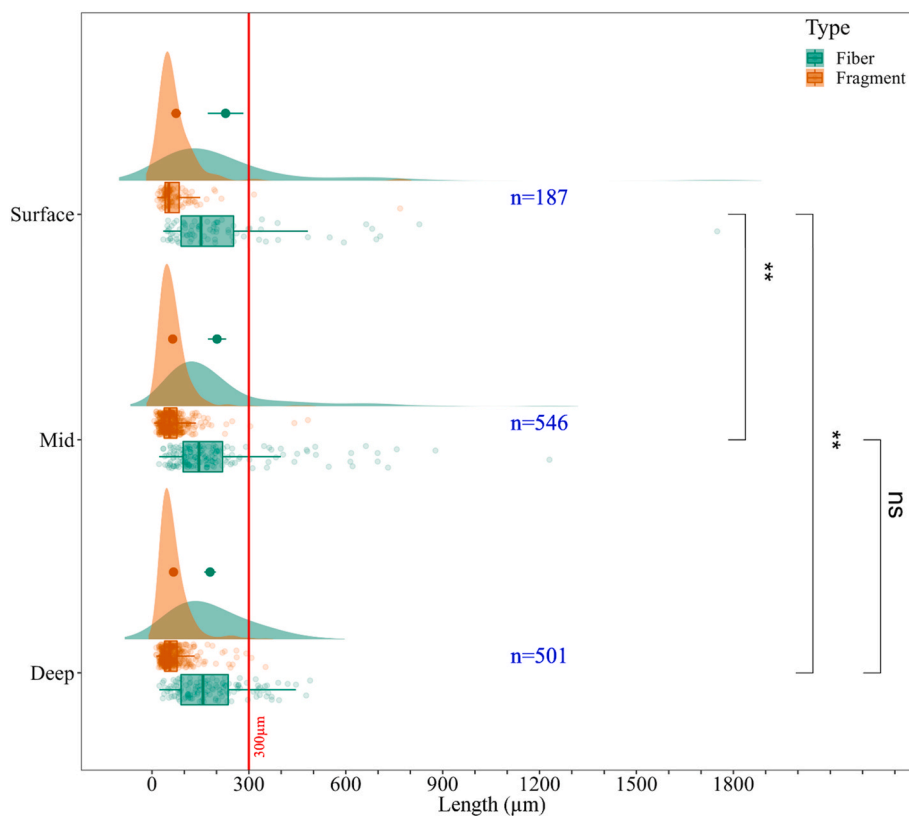


Fig. 5. The length distribution of the MP fibers and fragments in the surface, mid, and deep water. “Raincloud plots” (Allen et al., 2019) visualize raw data (points), length-frequency distribution (density), key summary statistics of the median, interquartile range (boxplot), and Kruskal-Wallis test between the lengths of samples where, ns: no significant,  $p > 0.05$ , \*:  $p \leq 0.05$ , \*\*:  $p \leq 0.01$ , \*\*\*:  $p \leq 0.001$ , \*\*\*\*:  $p \leq 0.0001$ .

of MPs in the ocean. For instance, bacterial biofilms growing on the surfaces of MPs can impact their density, weight, and surface characteristics, affecting their sinking rates and promoting their aggregation (Zettler et al., 2013; Kooi et al., 2017; Rummel et al., 2017). Ingestion of MPs by organisms (Cole et al., 2016) or aggregation of MPs into organic detritus (Summers et al., 2018), like marine snow, can promote the export of MPs from the surface to deep waters (Porter et al., 2018; Galgani et al., 2022).

#### 4.3. Effect of MPs characteristics on their vertical distribution in marine waters

The sinking rates and vertical distribution of MPs can be influenced by the characteristics of the MPs such as density and size. Low-density polymers contribute significantly to global plastic production and should theoretically be buoyant (Geyer et al., 2017). While it was previously expected that low-density MPs would predominantly accumulate in surface waters, a recent study by Eo et al. (2021) suggested that as much as 73% of total MPs in the water column were high-density polymers. In our study we similarly observed that high-density polymers constituted a larger share (68%) of the MPs compared to the low-density polymers (32%) across all depths. This indicates no direct connection between the density of MPs and their vertical distribution within the water column (Int-Veen et al., 2021). Most of the MPs found in this study were smaller than 300  $\mu\text{m}$ , as previously found in other areas in surface waters (Rist et al., 2020). The average size of MPs did not statistically differ among water layers. Small MPs (<100  $\mu\text{m}$ ) are expected to have a longer sinking time from the surface to deeper waters (Galgani et al., 2022) but are more likely to be trapped within biogenic aggregates (Cole et al., 2016; Porter et al., 2018; Bergami et al., 2020; Nava and Leoni, 2021), leading to their removal from the water column as part of marine snow (Cole et al., 2016; Porter et al., 2018). The

aggregation and sinking of MPs as part of the marine snow may explain how small low-density MPs sink at similar rates as high-density MPs, resulting in a lack of relationship between MP density and depth distribution, as observed here.

This finding is corroborated by several previous studies that have identified low-density small MPs in deep-sea sediments. For instance, in the Southern North Sea, polypropylene was the most prevalent polymer in sediments (Lorenz et al., 2019). Similarly, a sediment core from Balearic Sea exhibited a high abundance of polypropylene and polyethylene alongside polystyrene (Simon-Sánchez et al., 2022). The abyssal and hadal sediments of the Kuril Kamchatka trench also showed a high prevalence of polypropylene (Abel et al., 2021). Additionally, polypropylene was ranked among the six most frequent polymers in the sediment from Byfjorden Fjord, Norway (Haave et al., 2019) and in sediment from the Fram Strait (Tekman et al., 2020).

#### 4.4. Polymer composition, shape, and size

We examined the diversity of polymers present in the water samples. A total of 21 different polymer types were detected, comparable to other studies in the Baltic Sea areas (Uurasjärvi et al., 2021; Zhou et al., 2021; Zobkov et al., 2019). Eo et al. (2021) found 35 synthetic polymer types in samples collected in the South Korean continental shelf and deep sea area. The three dominant polymers were polyester, polypropylene, and polyethylene, which aligned with the results of other studies in different regions. For instance, in Southern Ocean, South Georgia, polyester was found to be the most polymer type abundant across all depths, followed by polypropylene (Rowlands et al., 2023). In the Gulf of Finland, polyethylene and polypropylene accounted for 73% of the identified polymers (Uurasjärvi et al., 2021), while in the Baltic Sea, the dominant polymers were polyethylene terephthalate, polyethylene, and polypropylene (Zobkov et al., 2019). According to Erni-Cassola et al. (2019),

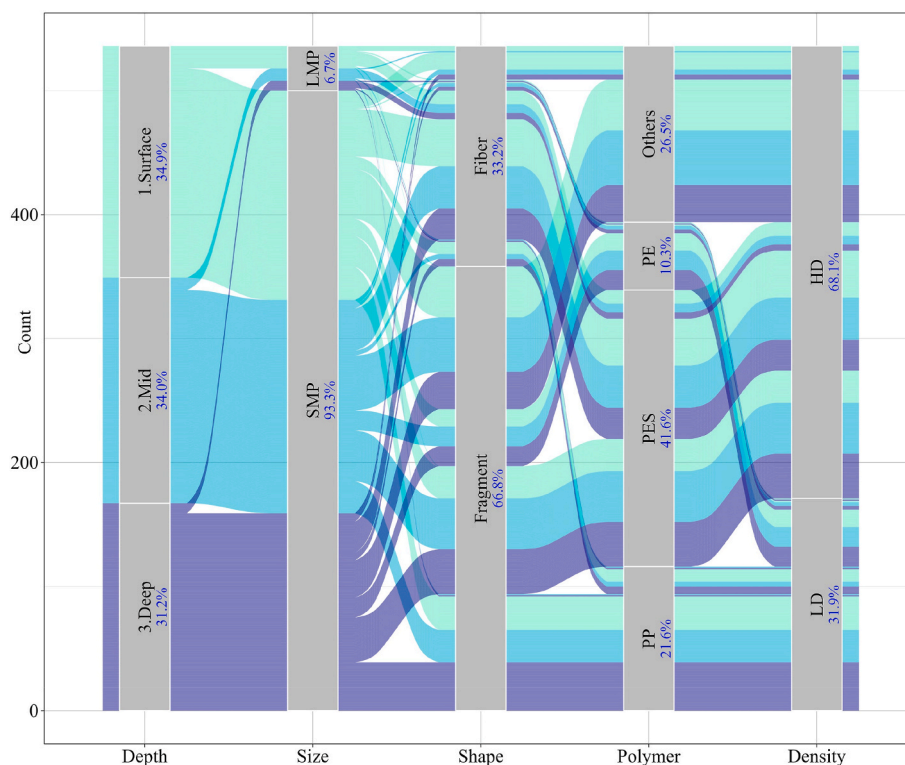


**Fig. 6.** The alluvial plot illustrates the characteristics of MPs across the different depths of water column encompassing size, shape, polymer, and the density at various sampling locations. Vertical sizes of the blocks and the widths of the alluvia are proportional to the counts. In this plot, the deep layer samples are depicted by dark blue color spline (alluvium), the mid layer samples are shown in light blue, and the surface layer samples are represented by light green. The thickness of the splines correspond to the percentage of their respective stratum. (For interpretation of the references to color in this figure legend, the reader is referred to the Web version of this article.)

low-density polymers like polypropylene and polyethylene were found at higher concentrations at the surface, and high-density polymers like polystyrene and acrylics were found at higher concentrations in deeper waters. However, in our study, we found that the dominant polymers, whether they were low-density or high-density, remained consistent across different water layers. Nevertheless, we observed the highest diversity in polymer composition in mid- and deep waters at certain stations (Table S1). Ultimately, the findings suggest that low-density polymers end up in the sediments, supporting the idea that material density alone does not solely determine the vertical distribution of MPs; instead, various complex interactions and processes are at play.

The shape of the MPs is also a factor influencing their vertical distribution (Kowalski et al., 2016; Khatmullina and Isachenko, 2017). Khatmullina and Isachenko, 2017 studied the settling velocity of variously shaped particles, including spheres, cylinders, and fishing lines, and revealed that the particle shape significantly affects their sinking rate. Liu et al., 2020 emphasized that fibrous and fragmented MPs accounted for over 90% of the total MPs in most studies, with fibers comprising the majority (ranging from 43 to 100%) of MPs particles. Interestingly, in our study, we observed that fragments were the prevailing form MPs at all depths, representing 70% of the MPs, which aligns with the findings of Song et al., 2018; Eo et al., 2021; Uurasjärvi et al., 2021, where fragments were also predominant. The effect of particle shape becomes significant only for particles of a specific size, namely larger particles where settling is highly influenced by their shape (Hazzab et al., 2008; Wang et al., 2021). However, for smaller particles with sizes less than 1 mm (equivalent spherical diameter), the shape has minimal impact on their sinking rates (Li et al., 2023).

A size-dependent removal mechanism was noted by Dai et al., 2018, who suggested that the proportion of fibrous MPs was lower in subsurface waters compared to surface samples, and the numerical proportion of MPs <300  $\mu\text{m}$  increased with depth. Similarly, Zobkov et al., 2019

reported an exponential decrease in MPs size with depth in the Baltic Sea. In our study, we found that MPs ranging in size from 11 to 100  $\mu\text{m}$  were dominant at all depths, and there were no significant differences among the depths. This suggests that the sinking velocity of small MPs is very low, causing them to disperse more widely throughout the water column; as a result, they remain in the water column without being trapped by the pycnocline (Zhao et al., 2022). Interestingly, particles less than <100  $\mu\text{m}$ , including MPs are much less influenced by stratification (Ardekani and Stocker, 2010; Doostmohammadi et al., 2012; More and Ardekani, 2023), which is consistent with our findings.

#### 4.5. Ecological implications

The accumulation of MPs in surface waters (e.g., marine litter windrows) can increase the risk of marine biota being exposed to plastic pollution (Cózar et al., 2021; Campillo et al., 2023). Similarly, pelagic organisms living or migrating in the water column can be exposed to subsurface layers of high concentrations of MPs, increasing the risk of ingestion or the toxic effects associated with plastic pollution in the deeper strata (Choy et al., 2019). For instance, the occurrence of MPs in mesopelagic organisms living at the depth of peaking plastic concentrations was observed to be 100% (Choy et al., 2019). There is increasing evidence that small MPs are incorporated into the marine snow (Zhao et al., 2018; Galgani et al., 2022). Marine snow can accumulate in very thin layers in the Baltic (e.g., 50–55 m) at the beginning of the pycnocline, attracting zooplankton (Möller et al., 2012) and increasing the risk of ingestion and exposure to MPs. However, our study did not find any accumulation layer of MPs. Further investigation on the role of marine snow aggregates in the distribution and bioavailability of MPs to pelagic organisms is needed.

Although the ingestion of MPs is relatively high for some pelagic organisms (e.g. fish, turtles, Duncan et al., 2019; Kühn and van



Franecker, 2020), the concentrations of MPs found in the water column in our study area were six orders of magnitude lower than those causing adverse effects on plankton based on laboratory exposure studies ( $>200$  MP mL<sup>-1</sup> for MPs, e.g., Cole et al., 2013; Lee et al., 2013; Setälä et al., 2014; Jeong et al., 2017; Vroom et al., 2017; Choi et al., 2020; Rodrigues et al., 2021). The mass of plastics found in the water column was in the order of  $\mu\text{g}$  of plastic per m<sup>3</sup>, which is several orders of magnitude lower than the mass of micronized plastics causing toxic leachates effects on plankton (Gunaalan et al., 2020; Cormier et al., 2021; Almeda et al., 2023). In general, with some local exceptions and independently of the sampling season, the MP concentration commonly found in marine waters is typically  $<1$  MPs L<sup>-1</sup>, which is in line with our findings. Therefore, our field data suggest a low risk of negative impacts of conventional MPs on the marine plankton food web in the Kattegat. However, it is important to note that there is a continuous export of MPs to the sediments/seafloor since MPs, regardless of their density, size, and shape, tend to sink (Woodall et al., 2014; Martin et al., 2022). Therefore, benthic organisms may potentially be exposed to higher levels of plastic pollution than planktonic organisms.

## 5. Conclusions

The present study is the first investigation of the vertical distribution and features of MPs in Danish waters. Our results show that MPs are ubiquitous in the water column in the studied area, with an average concentration of 53 MPs m<sup>-3</sup> and 47 MPs m<sup>-3</sup> at mid and deep waters respectively. Small plastic fragments ( $<300$   $\mu\text{m}$ ) of high-density polymers were the dominant MPs across all depths examined. No trend was observed between the concentration or polymer composition of MPs and the density of the water masses despite the strong stratification.

## Author statement

Kuddithamby Gunaalan: laboratory and data analysis, methodological application, writing - original draft, graphical representations. Rodrigo Almeda: conceptualization, supervision, writing - review & editing, resources, funding acquisition. Alvise Vianello: methodological application, supervision, writing - review & editing. Claudia Lorenz: methodological application, supervision, writing - review & editing. Lucian Iordachescu: methodological application, review & editing. Konstantinos Papacharalampos: methodological application, review & editing. Torkel Gissel Nielsen: conceptualization, supervision, writing - review & editing, resources, funding acquisition. Jes Vollertsen: conceptualization, supervision, writing - review & editing, resources, funding acquisition.

## Declaration of competing interest

The authors declare that they have no known competing financial interests or personal relationships that could have appeared to influence the work reported in this paper.

## Data availability

Data will be made available on request.

## Acknowledgement

We express our thanks to the crew of the R/V DANA, as well as to Christian Mathias Rohde Kiær and Asbjørn Haaning Nielsen for their assistance during the sampling process. Additionally, we extend our gratitude to María Sobrino Blanco for support in preparing the samples. Furthermore, we thank the RESPONSE project founded by (JPI Oceans, through the national funding agency of Denmark (Innovation Fund-Denmark), the Velux Foundation for the financial support through the project MarinePlastic (Project no. 25084), the ULPGC- Science and

Technology Park Foundation (agreement DTU-ULPGC, C2020/65), the Spanish Ministry of Science and Innovation through the MICROPLEACH project (PID2020-120479 GA-I00) and a Ramón y Cajal Program grant (RYC2018-025770-I) to RA.

## Appendix A. Supplementary data

Supplementary data to this article can be found online at <https://doi.org/10.1016/j.envpol.2023.122865>.

## References

- Abel, S.M., Primpke, S., Int-Veen, I., Brandt, A., Gerdt, G., 2021. Systematic identification of microplastics in abyssal and hadal sediments of the Kuril Kamchatka trench. *Environmental Pollution* 269, 116095. <https://doi.org/10.1016/j.envpol.2020.116095>.
- Allen, M., Poggiali, D., Whitaker, K., Marshall, T.R., Kievit, R.A., 2019. Raincloud plots: a multi-platform tool for robust data visualization. *Wellcome Open Res.* 4, 63. <https://doi.org/10.12688/wellcomeopenres.15191.1>.
- Almeda, R., Gunaalan, K., Alonso-López, O., Vilas, A., Clérandeau, C., Loisel, T., Nielsen, T.G., Cachot, J., Beiras, R., 2023. A protocol for lixiviation of micronized plastics for aquatic toxicity testing. *Chemosphere* 333, 138894. <https://doi.org/10.1016/j.chemosphere.2023.138894>.
- Ardekani, A.M., Stocker, R., 2010. Stratlets: low Reynolds number point-force solutions in a stratified fluid. *Phys. Rev. Lett.* 105, 084502. <https://doi.org/10.1103/PhysRevLett.105.084502>.
- Bendtsen, J., Gustafsson, K.E., Söderkvist, J., Hansen, J.L.S., 2009. Ventilation of bottom water in the North sea-baltic sea transition zone. *J. Mar. Syst.* 75, 138–149. <https://doi.org/10.1016/j.jmarsys.2008.08.006>.
- Bergami, E., Manno, C., Cappello, S., Vannuccini, M.L., Corsi, I., 2020. Nanoplastics affect moulting and faecal pellet sinking in Antarctic krill (*Euphausia superba*) juveniles. *Environ. Int.* 143, 105999. <https://doi.org/10.1016/j.envint.2020.105999>.
- Borges-Ramírez, M.M., Mendoza-Franco, E.F., Escalona-Segura, G., Osten, J.R., 2020. Plastic density as a key factor in the presence of microplastic in the gastrointestinal tract of commercial fishes from Campeche Bay, Mexico. *Environ. Pollut.* 267, 115659. <https://doi.org/10.1016/j.envpol.2020.115659>.
- Brach, L., Deixonne, P., Bernard, M.-F., Durand, E., Desjean, M.-C., Perez, E., van Sebille, E., ter Halle, A., 2018. Anticyclonic eddies increase accumulation of microplastic in the North Atlantic subtropical gyre. *Mar. Pollut. Bull.* 126, 191–196. <https://doi.org/10.1016/j.marpolbul.2017.10.077>.
- Campillo, A., Almeda, R., Vianello, A., Gómez, M., Martínez, I., Navarro, A., Herrera, A., 2023. Searching for hotspots of neustonic microplastics in the Canary Islands. *Mar. Pollut. Bull.* 192, 115057. <https://doi.org/10.1016/j.marpolbul.2023.115057>.
- Choi, J.S., Hong, S.H., Park, J.-W., 2020. Evaluation of microplastic toxicity in accordance with different sizes and exposure times in the marine copepod *Tigriopus japonicus*. *Mar. Environ. Res.* 153, 104838. <https://doi.org/10.1016/j.marenvres.2019.104838>.
- Choy, C.A., Robison, B.H., Gagne, T.O., Erwin, B., Firl, E., Halden, R.U., Hamilton, J.A., Katija, K., Lisin, S.E., Rolsky, C., Van Houtan K. S., 2019. The vertical distribution and biological transport of marine microplastics across the epipelagic and mesopelagic water column. *Sci. Rep.* 9, 7843. <https://doi.org/10.1038/s41598-019-44117-2>.
- Cole, M., Lindeque, P., Fileman, E., Halsband, C., Goodhead, R., Moger, J., Galloway, T. S., 2013. Microplastic ingestion by zooplankton. *Environ. Sci. Technol.* 47, 6646–6655. <https://doi.org/10.1021/es400663f>.
- Cole, M., Lindeque, P.K., Fileman, E., Clark, J., Lewis, C., Halsband, C., Galloway, T.S., 2016. Microplastics alter the properties and sinking rates of zooplankton faecal pellets. *Environ. Sci. Technol.* 50, 3239–3246. <https://doi.org/10.1021/acs.est.5b05905>.
- Cormier, B., Gambardella, C., Tato, T., Perdriat, Q., Costa, E., Veclin, C., Le Bihanic, F., Grassl, B., Dubocq, F., Kärrman, A., Van Arkel, K., Lemoine, S., Lagarde, F., Morin, B., Garaventa, F., Faimali, M., Cousin, X., Bégout, M.-L., Beiras, R., Cachot, J., 2021. Chemicals sorbed to environmental microplastics are toxic to early life stages of aquatic organisms. *Ecotoxicol. Environ. Saf.* 208, 111665. <https://doi.org/10.1016/j.ecoenv.2020.111665>.
- Cózar, A., Aliani, S., Basurko, O.C., Arias, M., Isobe, A., Topouzelis, K., Rubio, A., Morales-Caselles, C., 2021. Marine litter windrows: a strategic target to understand and manage the ocean plastic pollution. *Front. Mar. Sci.* 8. <https://doi.org/10.3389/fmars.2021.571796>.
- Cózar, A., Echevarría, F., González-Gordillo, J.I., Irigoien, X., Úbeda, B., Hernández-León, S., Palma, A.T., Navarro, S., García-de-Lomas, J., Ruiz, A., Fernández-de-Puelles, M.L., Duarte, C.M., 2014. Plastic debris in the open ocean. *Proc. Natl. Acad. Sci. U.S.A.* 111, 10239–10244. <https://doi.org/10.1073/pnas.1314705111>.
- Cressey, D., 2016. Bottles, bags, ropes and toothbrushes: the struggle to track ocean plastics. *Nature* 536, 263–265. <https://doi.org/10.1038/536263a>.
- Dai, Z., Zhang, H., Zhou, Q., Tian, Y., Chen, T., Tu, C., Fu, C., Luo, Y., 2018. Occurrence of microplastics in the water column and sediment in an inland sea affected by intensive anthropogenic activities. *Environ. Pollut.* 242, 1557–1565. <https://doi.org/10.1016/j.envpol.2018.07.131>.
- Díez-Minguito, M., Bermúdez, M., Gago, J., Carretero, O., Viñas, L., 2020. Observations and idealized modelling of microplastic transport in estuaries: the exemplary case of

- an upwelling system (Ría de Vigo, NW Spain). *Mar. Chem.* 222, 103780 <https://doi.org/10.1016/j.marchem.2020.103780>.
- Doostmohammadi, A., Stocker, R., Ardekani, A.M., 2012. Low-Reynolds-number swimming at pycnoclines. *Proc. Natl. Acad. Sci. U. S. A.* 109, 3856–3861. <https://doi.org/10.1073/pnas.1116210109>.
- Doyle, M.J., Watson, W., Bowlin, N.M., Sheavly, S.B., 2011. Plastic particles in coastal pelagic ecosystems of the Northeast Pacific ocean. *Mar. Environ. Res.* 71, 41–52. <https://doi.org/10.1016/j.marenvres.2010.10.001>.
- Duncan, E.M., Broderick, A.C., Fuller, W.J., Galloway, T.S., Godfrey, M.H., Hamann, M., Limpus, C.J., Lindeque, P.K., Mayes, A.G., Omeyer, L.C.M., Santillo, D., Snape, R.T.E., Godley, B.J., 2019. Microplastic ingestion ubiquitous in marine turtles. *Global Change Biol.* 25, 744–752. <https://doi.org/10.1111/gcb.14519>.
- Eo, S., Hong, S.H., Song, Y.K., Han, G.M., Seo, S., Shim, W.J., 2021. Prevalence of small high-density microplastics in the continental shelf and deep sea waters of East Asia. *Water Res.* 200, 117238 <https://doi.org/10.1016/j.watres.2021.117238>.
- Eriksen, M., Lebreton, L.C.M., Carson, H.S., Thiel, M., Moore, C.J., Borroero, J.C., Galgani, F., Ryan, P.G., Reisser, J., 2014. Plastic pollution in the world's oceans: more than 5 trillion plastic pieces weighing over 250,000 tons afloat at sea. *PLoS One* 9, e111913. <https://doi.org/10.1371/journal.pone.0111913>.
- Erni-Cassola, G., Zadjelovic, V., Gibson, M.I., Christie-Oleza, J.A., 2019. Distribution of plastic polymer types in the marine environment; A meta-analysis. *J. Hazard Mater.* 369, 691–698. <https://doi.org/10.1016/j.jhazmat.2019.02.067>.
- Fagiano, V., Compa, M., Alomar, C., Rios-Fuster, B., Morató, M., Capó, X., Deudero, S., 2023. Breaking the paradigm: marine sediments hold two-fold microplastics than sea surface waters and are dominated by fibers. *Sci. Total Environ.* 858, 159722 <https://doi.org/10.1016/j.scitotenv.2022.159722>.
- Galgani, L., Goßmann, L., Scholz-Böttcher, B., Jiang, X., Liu, Z., Scheidemann, L., Schlundt, C., Engel, A., 2022a. Hitchhiking into the deep: how microplastic particles are exported through the biological carbon pump in the North Atlantic ocean. *Environ. Sci. Technol.* 56, 15638–15649. <https://doi.org/10.1021/acs.est.2c04712>.
- Geyer, R., Jambeck, J.R., Law, K.L., 2017. Production, use, and fate of all plastics ever made. *Sci. Adv.* 3, e1700782 <https://doi.org/10.1126/sciadv.1700782>.
- Gunaalan, K., Almeda, R., Lorenz, C., Vianello, A., Iordachescu, L., Papacharalampos, K., Rohde Kier, C.M., Vollertsen, J., Nielsen, T.G., 2023. Abundance and distribution of microplastics in surface waters of the Kattegat/Skagerrak (Denmark). *Environ. Pollut.* 318, 120853 <https://doi.org/10.1016/j.envpol.2022.120853>.
- Gunaalan, K., Fabbri, E., Capolupo, M., 2020. The hidden threat of plastic leachates: a critical review on their impacts on aquatic organisms. *Water Res.* 184, 116170 <https://doi.org/10.1016/j.watres.2020.116170>.
- Gunaalan, K., Nielsen, T.G., Rodríguez Torres, R., Lorenz, C., Vianello, A., Andersen, C. A., Vollertsen, J., Almeda, R., 2023b. Is zooplankton an entry point of microplastics into the marine food web? *Environ. Sci. Technol.* <https://doi.org/10.1021/acs.est.3c02575>.
- Haave, M., Lorenz, C., Primpke, S., Gerdt, G., 2019. Different stories told by small and large microplastics in sediment - first report of microplastic concentrations in an urban recipient in Norway. *Mar. Pollut. Bull.* 141, 501–513. <https://doi.org/10.1016/j.marpolbul.2019.02.015>.
- Hazzab, A., Terfous, A., Ghenaïm, A., 2008. Measurement and modeling of the settling velocity of isometric particles. *Powder Technol.* 184, 105–113. <https://doi.org/10.1016/j.powtec.2007.08.009>.
- Int, Veen, I., Nogueira, P., Isigkeit, J., Hanel, R., Kammann, U., 2021. Positively buoyant but sinking: polymer identification and composition of marine litter at the seafloor of the North Sea and Baltic Sea. *Mar. Pollut. Bull.* 172, 112876 <https://doi.org/10.1016/j.marpolbul.2021.112876>.
- Isobe, A., Uchiyama-Matsumoto, K., Uchida, K., Tokai, T., 2017. Microplastics in the Southern Ocean. *Mar. Pollut. Bull.* 114, 623–626. <https://doi.org/10.1016/j.marpolbul.2016.09.037>.
- Jeong, C.-B., Kang, H.-M., Lee, M.-C., Kim, D.-H., Han, J., Hwang, D.-S., Souissi, S., Lee, S.-J., Shin, K.-H., Park, H.G., Lee, J.-S., 2017. Adverse effects of microplastics and oxidative stress-induced MAPK/Nrf2 pathway-mediated defense mechanisms in the marine copepod *Paracyclopina nana*. *Sci. Rep.* 7, 41323 <https://doi.org/10.1038/srep41323>.
- Kanhai, L.D.K., Gärdfeldt, K., Lyashevskaya, O., Hassellöv, M., Thompson, R.C., O'Connor, I., 2018. Microplastics in sub-surface waters of the arctic central basin. *Mar. Pollut. Bull.* 130, 8–18. <https://doi.org/10.1016/j.marpolbul.2018.03.011>.
- Khatmullina, L., Isachenko, I., 2017. Settling velocity of microplastic particles of regular shapes. *Mar. Pollut. Bull.* 114, 871–880. <https://doi.org/10.1016/j.marpolbul.2016.11.024>.
- Kooi, M., Nes, E.H. van, Scheffer, M., Koelmans, A.A., 2017. Ups and downs in the ocean: effects of biofouling on vertical transport of microplastics. *Environ. Sci. Technol.* 51, 7963–7971. <https://doi.org/10.1021/acs.est.6b04702>.
- Kowalski, N., Reichardt, A.M., Waniek, J.J., 2016. Sinking rates of microplastics and potential implications of their alteration by physical, biological, and chemical factors. *Mar. Pollut. Bull.* 109, 310–319. <https://doi.org/10.1016/j.marpolbul.2016.05.064>.
- Kühn, S., van Franeker, J.A., 2020. Quantitative overview of marine debris ingested by marine megafauna. *Mar. Pollut. Bull.* 151, 110858 <https://doi.org/10.1016/j.marpolbul.2019.110858>.
- Kvale, K., Prowe, A.E.F., Chien, C.-T., Landolfi, A., Oschlies, A., 2020. The global biological microplastic particle sink. *Sci. Rep.* 10, 16670 <https://doi.org/10.1038/s41598-020-72898-4>.
- Kvale, K.F., Friederike Prowe, A.E., Oschlies, A., 2020. A critical examination of the role of marine snow and zooplankton fecal pellets in removing ocean surface microplastic. *Front. Mar. Sci.* 6.
- Law, K.L., Morét-Ferguson, S., Maximenko, N.A., Proskurowski, G., Peacock, E.E., Hafner, J., Reddy, C.M., 2010. Plastic accumulation in the North Atlantic subtropical gyre. *Science* 329, 1185–1188. <https://doi.org/10.1126/science.1192321>.
- Lee, K.-W., Shim, W.J., Kwon, O.Y., Kang, J.-H., 2013. Size-dependent effects of micro polystyrene particles in the marine copepod *Tigriopus japonicus*. *Environ. Sci. Technol.* 47, 11278–11283. <https://doi.org/10.1021/es401932b>.
- Lehmann, A., Myrberg, K., Post, P., Chubarenko, I., Dailidiene, I., Hinrichsen, H.-H., Hüsey, K., Liblik, T., Meier, H.E.M., Lips, U., Bukanova, T., 2022. Salinity dynamics of the Baltic Sea. *Earth Syst. Dynam.* 13, 373–392. <https://doi.org/10.5194/esd-13-373-2022>.
- Li, J., Shan, E., Zhao, J., Teng, J., Wang, Q., 2023. The factors influencing the vertical transport of microplastics in marine environment: a review. *Sci. Total Environ.* 870, 161893 <https://doi.org/10.1016/j.scitotenv.2023.161893>.
- Liu, F., Olesen, K.B., Borregaard, A.R., Vollertsen, J., 2019. Microplastics in urban and highway stormwater retention ponds. *Sci. Total Environ.* 671, 992–1000. <https://doi.org/10.1016/j.scitotenv.2019.03.416>.
- Liu, K., Courtene-Jones, W., Wang, X., Song, Z., Wei, N., Li, D., 2020. Elucidating the vertical transport of microplastics in the water column: a review of sampling methodologies and distributions. *Water Res.* 186, 116403 <https://doi.org/10.1016/j.watres.2020.116403>.
- Liu, Y., Lorenz, C., Vianello, A., Syberg, K., Nielsen, A.H., Nielsen, T.G., Vollertsen, J., 2023. Exploration of occurrence and sources of microplastics (>10 µm) in Danish marine waters. *Sci. Total Environ.* 865, 161255 <https://doi.org/10.1016/j.scitotenv.2022.161255>.
- Lorenz, C., Roscher, L., Meyer, M.S., Hildebrandt, L., Prume, J., Löder, M.G.J., Primpke, S., Gerdt, G., 2019. Spatial distribution of microplastics in sediments and surface waters of the southern North Sea. *Environ. Pollut.* 252, 1719–1729. <https://doi.org/10.1016/j.envpol.2019.06.093>.
- Martin, C., Young, C.A., Valluzzi, L., Duarte, C.M., 2022. Ocean sediments as the global sink for marine micro- and mesoplastics. *Limnology and Oceanography Letters* 7, 235–243. <https://doi.org/10.1002/lo2.10257>.
- Matthews, J.B.L., Buchholz, F., Saborowski, R., Tarling, G.A., Dallot, S., Labat, J.P., 1999. On the physical oceanography of the Kattegat and Clyde Sea area, 1996–98, as background to ecophysiological studies on the planktonic crustacean, *Meganactiphanes norvegica* (Euphausiacea). *Helgol. Mar. Res.* 53, 70–84. <https://doi.org/10.1007/PL00012140>.
- Michels, J., Stippkugel, A., Lenz, M., Wirtz, K., Engel, A., 2018. Rapid aggregation of biofilm-covered microplastics with marine biogenic particles. *Proc. Biol. Sci.* 285, 20181203 <https://doi.org/10.1098/rspb.2018.1203>.
- Möller, K.O., John, M.S., Temming, A., Floeter, J., Sell, A.F., Herrmann, J.-P., Möllmann, C., 2012. Marine snow, zooplankton and thin layers: indications of a trophic link from small-scale sampling with the Video Plankton Recorder. *Mar. Ecol. Prog. Ser.* 468, 57–69. <https://doi.org/10.3354/meps09984>.
- More, R.V., Ardekani, A.M., 2023. Motion in stratified fluids. *Annu. Rev. Fluid Mech.* 55, 157–192. <https://doi.org/10.1146/annurev-fluid-120720-011132>.
- Nava, V., Leoni, B., 2021. A critical review of interactions between microplastics, microalgae and aquatic ecosystem function. *Water Res.* 188, 116476 <https://doi.org/10.1016/j.watres.2020.116476>.
- Ni, S., Lu, Z., Zhang, Q., Groeneveld, J., Knudsen, K.L., Seidenkrantz, M.-S., Filipsson, H. L., 2023. Last interglacial seasonal hydroclimate in the North sea-baltic sea region. *Quat. Sci. Rev.* 312, 108152 <https://doi.org/10.1016/j.quascirev.2023.108152>.
- Nielsen, M.H., 2005. The baroclinic surface currents in the Kattegat. *J. Mar. Syst.* 55, 97–121. <https://doi.org/10.1016/j.jmarsys.2004.08.004>.
- Parać, M., Cuculić, V., Cukrov, Nuša, Geček, S., Lovrić, M., Cukrov, Neven, 2022. Microplastic distribution through the salinity gradient in a stratified estuary. *Water* 14, 3255. <https://doi.org/10.3390/w14203255>.
- Pasquier, G., Doyen, P., Kazour, M., Dehaut, A., Diop, M., Duflos, G., Amara, R., 2022. Manta net: the golden method for sampling surface water microplastics in aquatic environments. *Front. Environ. Sci.* 10.
- Pedersen, F.B., 1993. Fronts in the Kattegat: the hydrodynamic regulating factor for biology. *Estuaries* 16, 104–112. <https://doi.org/10.2307/1352768>.
- Porter, A., Lyons, B.P., Galloway, T.S., Lewis, C., 2018. Role of marine snows in microplastic fate and bioavailability. *Environ. Sci. Technol.* 52, 7111–7119. <https://doi.org/10.1021/acs.est.8b01000>.
- Primpke, S., Cross, R.K., Mintenig, S.M., Simon, M., Vianello, A., Gerdt, G., Vollertsen, J., 2020. Toward the systematic identification of microplastics in the environment: evaluation of a new independent software tool (SIMPLE) for spectroscopic analysis. *Appl. Spectrosc.* 74, 1127–1138. <https://doi.org/10.1177/0003702820917760>.
- Reisser, J., Slat, B., Noble, K., du Plessis, K., Epp, M., Proietti, M., de Sonneville, J., Becker, T., Pattiaratchi, C., 2015. The vertical distribution of buoyant plastics at sea: an observational study in the North Atlantic Gyre. *Biogeosciences* 12, 1249–1256. <https://doi.org/10.5194/bg-12-1249-2015>.
- Richardson, K., 1996. Carbon flow in the water column case study: the southern Kattegat. In: *Eutrophication in Coastal Marine Ecosystems*. American Geophysical Union (AGU), pp. 95–114. <https://doi.org/10.1029/CE052p0095>.
- Rist, S., Vianello, A., Winding, M.H.S., Nielsen, T.G., Almeda, R., Torres, R.R., Vollertsen, J., 2020. Quantification of plankton-sized microplastics in a productive coastal Arctic marine ecosystem. *Environ. Pollut.* 266, 115248 <https://doi.org/10.1016/j.envpol.2020.115248>.
- Rodrigues, S.M., Elliott, M., Almeida, C.M.R., Ramos, S., 2021. Microplastics and plankton: knowledge from laboratory and field studies to distinguish contamination from pollution. *J. Hazard Mater.* 417, 126057 <https://doi.org/10.1016/j.jhazmat.2021.126057>.
- Rowlands, E., Galloway, T., Cole, M., Peck, V.L., Posacka, A., Thorpe, S., Manno, C., 2023. Vertical flux of microplastic, a case study in the Southern Ocean, South

- Georgia. Mar. Pollut. Bull. 193, 115117 <https://doi.org/10.1016/j.marpolbul.2023.115117>.
- Rummel, C.D., Jahnke, A., Gorokhova, E., Kühnel, D., Schmitt-Jansen, M., 2017. Impacts of biofilm formation on the fate and potential effects of microplastic in the aquatic environment. Environ. Sci. Technol. Lett. 4, 258–267. <https://doi.org/10.1021/acs.estlett.7b00164>.
- Setälä, O., Fleming-Lehtinen, V., Lehtiniemi, M., 2014. Ingestion and transfer of microplastics in the planktonic food web. Environ. Pollut. 185, 77–83. <https://doi.org/10.1016/j.envpol.2013.10.013>.
- Setälä, O., Magnusson, K., Lehtiniemi, M., Norén, F., 2016. Distribution and abundance of surface water microlitter in the Baltic Sea: a comparison of two sampling methods. Mar. Pollut. Bull. 110, 177–183. <https://doi.org/10.1016/j.marpolbul.2016.06.065>.
- Shamskhany, A., Li, Z., Patel, P., Karimpour, S., 2021. Evidence of microplastic size impact on mobility and transport in the marine environment: a review and synthesis of recent research. Front. Mar. Sci. 8.
- Simon, M., van Alst, N., Vollertsen, J., 2018. Quantification of microplastic mass and removal rates at wastewater treatment plants applying Focal Plane Array (FPA)-based Fourier Transform Infrared (FT-IR) imaging. Water Res. 142, 1–9. <https://doi.org/10.1016/j.watres.2018.05.019>.
- Simon-Sánchez, L., Grelaud, M., Lorenz, C., Garcia-Orellana, J., Vianello, A., Liu, F., Vollertsen, J., Ziveri, P., 2022. Can a sediment core reveal the plastic age? Microplastic preservation in a coastal sedimentary record. Environ. Sci. Technol. 56, 16780–16788. <https://doi.org/10.1021/acs.est.2c04264>.
- Song, Y.K., Hong, S.H., Eo, S., Jang, M., Han, G.M., Isobe, A., Shim, W.J., 2018. Horizontal and vertical distribution of microplastics in Korean coastal waters. Environ. Sci. Technol. 52, 12188–12197. <https://doi.org/10.1021/acs.est.8b04032>.
- Summers, S., Henry, T., Gutierrez, T., 2018. Agglomeration of nano- and microplastic particles in seawater by autochthonous and de novo-produced sources of expolymeric substances. Mar. Pollut. Bull. 130, 258–267. <https://doi.org/10.1016/j.marpolbul.2018.03.039>.
- Sun, X., Wang, T., Chen, B., Booth, A.M., Liu, S., Wang, R., Zhu, L., Zhao, X., Qu, K., Xia, Bin, 2021. Factors influencing the occurrence and distribution of microplastics in coastal sediments: from source to sink. J. Hazard Mater. 410, 124982 <https://doi.org/10.1016/j.jhazmat.2020.124982>.
- Tekman, M.B., Wekerle, C., Lorenz, C., Primpke, S., Hasemann, C., Gerdt, G., Bergmann, M., 2020. Tying up loose ends of microplastic pollution in the arctic: distribution from the sea surface through the water column to deep-sea sediments at the HAUSGARTEN observatory. Environ. Sci. Technol. 54, 4079–4090. <https://doi.org/10.1021/acs.est.9b06981>.
- Thompson, R.C., Olsen, Y., Mitchell, R.P., Davis, A., Rowland, S.J., John, A.W.G., McGonigle, D., Russell, A.E., 2004. Lost at sea: where is all the plastic? Science 304 (838), 838. <https://doi.org/10.1126/science.1094559>.
- Uurasjärvi, E., Pääkkönen, M., Setälä, O., Koistinen, A., Lehtiniemi, M., 2021. Microplastics accumulate to thin layers in the stratified Baltic Sea. Environ. Pollut. 268, 115700 <https://doi.org/10.1016/j.envpol.2020.115700>.
- Van Cauwenbergh, L., Vanreusel, A., Mees, J., Janssen, C.R., 2013. Microplastic pollution in deep-sea sediments. Environ. Pollut. 182, 495–499. <https://doi.org/10.1016/j.envpol.2013.08.013>.
- van Sebille, E., Wilcox, C., Lebreton, L., Maximenko, N., Hardesty, B.D., van Franeker, J. A., Eriksen, M., Siegel, D., Galgani, F., Law, K.L., 2015. A global inventory of small floating plastic debris. Environ. Res. Lett. 10, 124006 <https://doi.org/10.1088/1748-9326/10/12/124006>.
- Vega-Moreno, D., Abaroa-Pérez, B., Rein-Loring, P.D., Presas-Navarro, C., Fraile-Nuez, E., Machín, F., 2021. Distribution and transport of microplastics in the upper 1150 m of the water column at the eastern North Atlantic subtropical gyre, canary islands, Spain. Sci. Total Environ. 788, 147802 <https://doi.org/10.1016/j.scitotenv.2021.147802>.
- Vianello, A., Jensen, R.L., Liu, L., Vollertsen, J., 2019. Simulating human exposure to indoor airborne microplastics using a Breathing Thermal Manikin. Sci. Rep. 9, 8670. <https://doi.org/10.1038/s41598-019-45054-w>.
- Vroom, R.J.E., Koelmans, A.A., Besseling, E., Halsband, C., 2017. Aging of microplastics promotes their ingestion by marine zooplankton. Environ. Pollut. 231, 987–996. <https://doi.org/10.1016/j.envpol.2017.08.088>.
- Wang, Z., Dou, M., Ren, P., Sun, B., Jia, R., Zhou, Y., 2021. Settling velocity of irregularly shaped microplastics under steady and dynamic flow conditions. Environ. Sci. Pollut. Res. 28, 62116–62132. <https://doi.org/10.1007/s11356-021-14654-3>.
- Woodall, L.C., Sanchez-Vidal, A., Canals, M., Paterson, G.L.J., Coppock, R., Sleight, V., Calafat, A., Rogers, A.D., Narayanaswamy, B.E., Thompson, R.C., 2014. The Deep Sea Is a Major Sink for Microplastic Debris. vol. 1. Royal Society Open Science, 140317. <https://doi.org/10.1098/rsos.140317>.
- World Health Organization, 1997. Determination of Airborne Fibre Number Concentrations : a Recommended Method, by Phase-Contrast Optical Microscopy (Membrane Filter Method). World Health Organization.
- Wu, P., Huang, J., Zheng, Y., Yang, Y., Zhang, Y., He, F., Chen, H., Quan, G., Yan, J., Li, T., Gao, B., 2019. Environmental occurrences, fate, and impacts of microplastics. Ecotoxicol. Environ. Saf. 184 <https://doi.org/10.1016/j.ecoenv.2019.109612>.
- Zettler, E.R., Mincer, T.J., Amaral-Zettler, L.A., 2013. Life in the “plastisphere”: microbial communities on plastic marine debris. Environ. Sci. Technol. 47, 7137–7146. <https://doi.org/10.1021/es401288x>.
- Zhao, S., Mincer, T.J., Lebreton, L., Egger, M., 2023. Pelagic microplastics in the North Pacific Subtropical Gyre: a prevalent anthropogenic component of the particulate organic carbon pool. PNAS Nexus 2, pgad070. <https://doi.org/10.1093/pnasnexus/pgad070>.
- Zhao, S., Ward, J.E., Danley, M., Mincer, T.J., 2018. Field-based evidence for microplastic in marine aggregates and mussels: implications for trophic transfer. Environ. Sci. Technol. 52, 11038–11048. <https://doi.org/10.1021/acs.est.8b03467>.
- Zhao, S., Zettler, E.R., Bos, R.P., Lin, P., Amaral Zettler, L.A., Mincer, T.J., 2022. Large quantities of small microplastics permeate the surface ocean to abyssal depths in the South Atlantic Gyre. Global Change Biol. 28, 2991–3006. <https://doi.org/10.1111/gcb.16089>.
- Zhou, Q., Tu, C., Yang, J., Fu, C., Li, Y., Wanik, J.J., 2021. Trapping of microplastics in halocline and turbidity layers of the semi-enclosed Baltic Sea. Front. Mar. Sci. 8.
- Zobkov, M.B., Esiukova, E.E., Zyubin, A.Y., Samusev, I.G., 2019. Microplastic content variation in water column: the observations employing a novel sampling tool in stratified Baltic Sea. Mar. Pollut. Bull. 138, 193–205. <https://doi.org/10.1016/j.marpolbul.2018.11.047>.